

Article

Comparing the Effects of Green and Blue Bodies and Urban Morphology on Land Surface Temperatures Close to Rivers and Large Lakes

Vlad'ka Kirschner ^{1,*}, David Moravec ², Karel Macků ³, Giorgi Kozhoridze ² and Jan Komárek ²

¹ Department of Landscape and Urban Planning, Faculty of Environmental Sciences, Czech University of Life Sciences Prague, 16500 Prague, Czech Republic

² Department of Spatial Sciences, Faculty of Environmental Sciences, Czech University of Life Sciences Prague, 16500 Prague, Czech Republic

³ Department of Geoinformatics, Palacký University in Olomouc, 77900 Olomouc, Czech Republic

* Correspondence: kirschner@fzp.czu.cz

Abstract: Understanding the complex contributions of several factors to an urban heat island is crucial for assessing the impacts of planning on the thermal conditions within cities. It is relatively well-known how the different factors work separately, but how they work together, especially near water bodies, is still unclear. This paper investigates the effects of blue bodies (rivers or large lakes), the normalized difference vegetation index (NDVI), building coverage (BC), and building height (BH) on the land surface temperature (LST), comparing the situation around lakes and a river. Their inter-relationships are explored in a square grid of 30 × 30 m using Landsat-8 data on LST measurements in Prague, Czech Republic, in summer 2022. Multiple regression models are used for the analysis. The results imply that the NDVI significantly reduces LSTs, followed rivers if within 200 m of one, while the effect of lakes is negligible. The effect of BH is low. BC is a predominant factor in the city, generating a warming effect, which increases with the city's compactness. The main planning implications are to base urban heat island mitigation strategies on compensating for building coverage with live and dense green bodies, promoting vertical development.

Keywords: land surface temperature; Prague; NDVI



Citation: Kirschner, V.; Moravec, D.; Macků, K.; Kozhoridze, G.; Komárek, J. Comparing the Effects of Green and Blue Bodies and Urban Morphology on Land Surface Temperatures Close to Rivers and Large Lakes. *Land* **2024**, *13*, 162. <https://doi.org/10.3390/land13020162>

Academic Editors: Rajnish Kaur Calay, Lawrence Lau and Isaac Yu Fat Lun

Received: 15 December 2023

Revised: 20 January 2024

Accepted: 22 January 2024

Published: 30 January 2024



Copyright: © 2024 by the authors. Licensee MDPI, Basel, Switzerland. This article is an open access article distributed under the terms and conditions of the Creative Commons Attribution (CC BY) license (<https://creativecommons.org/licenses/by/4.0/>).

1. Introduction

Cities modify surface energy balances and typically exhibit higher temperatures than their surrounding rural areas; such an effect is well known as the urban heat island (UHI) effect. Many studies [1–4] have shown that the temperature increases with increased urban density and compactness. Nevertheless, dense and compact cities have been broadly recognized as sustainable [5], and as such, this urban format has been applied in many policies both in the European Union [6] and in other parts of the world [7]. With global climate change, the UHI effect has become a major challenge, especially in dense and compact cities, as it increases health (and even death) risks for urban residents [8].

In order to mitigate the negative impacts of urban warming, we must understand the effects of the factors contributing to the variability in climate conditions within cities. The land surface temperature (LST) obtained via remote sensing for an entire city seems better suited to describing this variability than the air temperature measured by a relatively coarse network of local weather stations [9]. LST is not the same as air temperature, but is closely related to the near-surface air temperature; it is considered a primary factor affecting the energy exchange of the near-surface layers of the atmosphere [10,11]. It accurately characterizes the thermal environment at the city scale [12], and it is widely used to assess the UHI effect. In this respect, we refer to the surface UHI (SUHI), associated with the “skin” temperature of the ground [11].

Currently, attention towards the contribution of nature-based solutions to address UHI challenges is growing, introducing green and blue infrastructure in nationwide and urban climate change adaptation and mitigation strategies [13,14]. Although many studies have reported the cooling effect of green and blue urban bodies [4,15–17], the magnitude of the effect of blue bodies remains relatively unclear [18,19]. In addition, the strategies must be based on local climate conditions [3] and specific urban morphology [1] to be effective. Among the studies addressing nature-based solutions and strategies, European conditions have been much less often studied than Asian ones [15,16,20–22].

Green bodies can have various urban forms, from public parks and street alleys to private gardens. Vegetation transfers energy from the urban surface to the atmosphere through water evaporation. This process, known as evapotranspiration, is the most commonly offered explanation for the cooling effect of greenery [4]. Since the water evaporates mainly through the leaves' surfaces, evapotranspiration is influenced by the size and type of the vegetation [23–25]. The normalized difference vegetation index (NDVI) was shown to be a good proxy for the density and condition (amount of chlorophyll) of vegetation, and is therefore widely used in SUHI studies [3,12,26]. Vegetation in good condition absorbs red radiation for photosynthesis while reflecting infrared radiation. With less chlorophyll for photosynthesis in vegetation, more red radiation is reflected, and the NDVI decreases.

As with green bodies, blue bodies are affected by the background climate, including local wind [4]; nevertheless, the primary cooling effect is due to evaporation [18,20]. Blue bodies within cities can have a dynamic character (rivers) or a static character (lakes); the water dynamics significantly influence the thermal conditions of the water [18]. The water is more permeable to short-wave radiation than soil (and other natural surfaces); the LST of water is, therefore, lower than that of soil. When the mixing of water occurs due to its dynamics, the water heat reserves are also mixed, and the thermal conditions of the water are much more stable than those of soil. As rivers show more dynamics than lakes, this may result in different effects of blue bodies on LST. For instance, rivers were associated with a lower cooling effect than lakes in the Pearl River Delta Metropolitan Region in China [20], while lakes in some European cities were reported to have only a slight cooling or even warming effect [18,19,27]. In addition, many studies confirm that only larger blue bodies have a noticeable cooling effect, which decreases with the distance from the water body [18,19]. Lin et al. [20] found that when the distance exceeded 200 m, blue bodies of 0.01 ha to 50 ha contributed non-significantly to differences in LST.

Few studies have compared the effect of green and blue bodies within cities, and their results are inconsistent. For example, green bodies were found to have a more significant cooling effect than blue bodies in Kolkata, India [16], while in northern China, the cooling effect of rivers was more substantial than that of local green bodies [28].

It is clear that urban morphology affects the LST, but the debate about the contribution of individual factors is ongoing [3]. Areas covered by buildings (i.e., building coverage, BC) and the height of the buildings (BH) constitute the most often mentioned factors influencing the LST [1,12,26,27,29]. It is clear that BC warms up the environment; this effect is explained by the fact that buildings, as impervious surfaces, have lower albedos and thus absorb more solar irradiation [1]. The degree of this effect, however, differs among cities. For example, BC warms up the environment more than BH in Dhaka, Bangladesh, or Guangzhou, China [12,30], whereas BH in Beijing influences the LST more than both BC and green bodies [29]. In addition, high-rise buildings can sometimes cool down their surroundings [12,29,31], which is explained by the shadows cast by such buildings [13,32]. In 25 European cities, the relationships between BH and LST were found to be weak and inconsistent (both positive and negative) [21]. In another study on four European cities, the LST increased with BHs up to 9 m, after which the effect was inconsistent [33].

It is necessary to investigate the effects of green and blue bodies in the context of urban morphology so that their cooling effect can be well utilized in urban planning. Nevertheless, current studies insufficiently cover this issue, particularly in the European climate. This study aims to compare the impacts of building height (BH), building coverage (BC), the

NDVI, proximity to lakes larger than 1000 m², and proximity to the river on the LST. We expect to find a cooling effect of the NDVI, and we intend to further investigate the local effect of blue bodies.

2. Materials and Methods

2.1. Study Area

The study area is located in the city of Prague, the capital of the Czech Republic (50°5' N, 14°25' E), a representative of a typical compact European city with high-density development as promoted by the European Commission [6,34]. The Czech Republic has a temperate climate, being situated on the border of the western oceanic climate and the eastern continental climate, with a typical cycle of four seasons [35]. Prague is situated within a temperate region in the center of the Czech Republic. The country has already been experiencing the effects of climate change; the average temperature in the Czech Republic has increased by 2 °C over the last 60 years, and it is predicted to increase by another 2 °C by 2050 [35]. The annual mean temperature in Prague in 2019 was 9.5 °C [36]. The average summer (June–August) temperature in 2019 was 19.5 °C, the highest average summer temperature since 1961. The average summer temperature increased mainly because of the increased temperature in June, which was particularly high in Prague (24.5 °C) [36]. Regarding annual precipitation, the year 2019 was typical for the region, with a total of 634 mm [36].

The study area covers the intersection of the administrative borders of Prague and the satellite image used for temperature measurement (Figure 1). A single satellite image was used to provide a set of comparable data. The measurement deviation (caused by, for example, the sky view factor) is negligible. The city of Prague was, for the purposes of this study, divided into three zones according to their location and spatial characteristics: the inner compact city, the outer compact city, and the outskirts (Figure 1). The zones were created for planning purposes, and their division is based on the borders defined by the 2009 Concept of Prague's Master Plan [37]. The inner compact city is characterized by block structures of mostly 4 to 6 floors, with pockets of parks. The outer compact city consists of both housing estates, with apartment buildings of typically 8 to 12 floors, and low-density family housing. Strips of greenery with scattered trees between the high-rise housing estates and the low-density residential areas are relatively common. The city's outskirts are characterized by suburban landscapes with clusters of low-density housing (Figure 2).

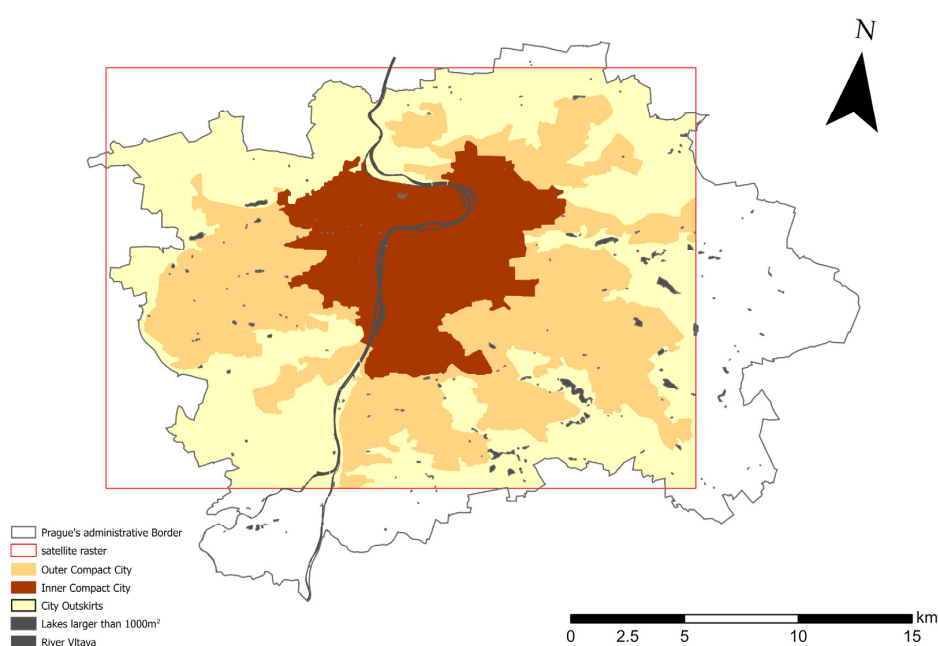


Figure 1. Study area—the city of Prague divided into three zones within the satellite raster.

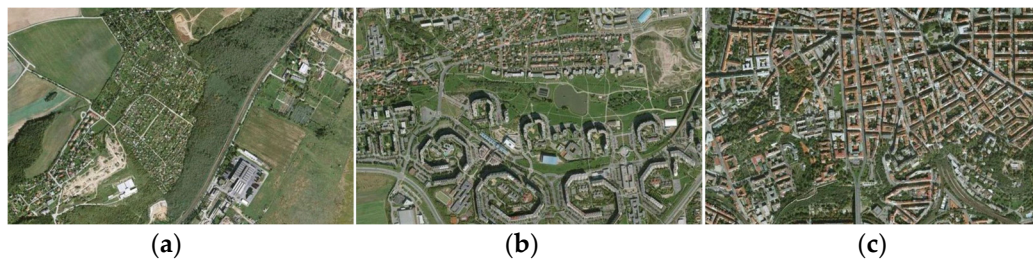


Figure 2. Spatial characteristics of the three zones of Prague used for the study: (a) city outskirts, (b) outer compact city, and (c) inner compact city. (Retrieved from mapy.cz).

2.2. Temperature Measurement

Similarly to many other studies [3,21,38], we used LST data collected by satellites. The LST data were derived from the Landsat-8 TIRS band 10 imagery, with a ground resolution of 100 m resampled to 30 m by the provider, corresponding to the maximum resolution of the Landsat-8 satellite bands. This resolution was chosen to best reflect the detail of Prague input data (i.e., data to calculate proximity to the river, proximity to lakes larger than 1000 m², BH, and BC). The image was acquired on 26 June 2019, at 11:50 a.m. local time, during peak solar activity, in clear atmospheric conditions, when the air temperature in the center of Prague (Karlovy weather station) was 31.2 °C, with a wind speed of 1.8 m s⁻¹ and a relative humidity of 47%. As the nighttime Landsat sensor image is missing for our location and date, only the image during peak solar activity (solar noon) is investigated in this study.

The surface temperature raster was obtained from the bottom of the atmosphere radiance in Landsat-8 band 10 following the procedure published by Barsi et al. [28,29]. In the first step, the digital number of the Landsat-8 band 10 was converted into the top-of-atmosphere spectral radiance, L_{TOA} , using the following equation:

$$L_{TOA} = M_L * DN + A_L, \quad (1)$$

where M_L is the band radiance multiplicative scaling factor, and A_L is the band radiance additive scaling factor (both available from the satellite imagery metadata).

After that, the L_{TOA} was converted into the bottom-of-atmosphere radiance, L_{BOA} , using the following equation:

$$L_{BOA} = \frac{L_{TOA} - L_u - \tau(1 - \epsilon)L_d}{\tau\epsilon}, \quad (2)$$

where τ is atmospheric transmission, L_u is the upwelling atmospheric path radiance, and L_d is the downwelling sky radiance. All three atmospheric parameters were obtained from the Atmospheric Correction Parameter Calculator, available online: <https://atmcorr.gsfc.nasa.gov/>, accessed on 1 July 2021. ϵ is the emissivity of the surface. The raster of emissivity was obtained from the NDVI raster according to the procedure proposed by Van De Griend and Owe [39] using the following equation:

$$\epsilon = 1.0094 + 0.047 \times \ln(\text{NDVI}). \quad (3)$$

2.3. Creating Input Data (Factors) for Analysis

Based on the findings of previous studies [12,20,29], five commonly used factors were selected as the independent variables: the normalized difference vegetation index (NDVI), proximity to lakes larger than 1000 m², proximity to the Vltava river, building coverage (BC), and building height (BH). The first of these, the NDVI, is regarded as the basic index for measuring the Earth's natural surfaces, particularly for measuring the health and quantity of vegetation. Technically, it is a linear combination of the near-infrared and red bands [40]. Healthy vegetation absorbs the red spectrum and reflects the near-infrared spectrum, which is expressed in NDVI values. The higher the quality and quantity of vegetation, the higher the index value. To obtain a precise NDVI raster, the Landsat-8

image was first atmospherically corrected in the ENVI 5.5 software using the FLAASH atmospheric correction method [41], and, subsequently, the NDVI raster with a resolution of 30 m was calculated using the following equation:

$$\text{NDVI} = \frac{\text{NIR} - \text{RED}}{\text{NIR} + \text{RED}}, \quad (4)$$

where NIR and RED are the reflectances of the near-infrared (band 5) and red (band 4) bands of the Landsat-8 imagery.

The data on BH, BC, the river, and lakes, as well as a digital surface model of the city of Prague, are freely available from the Prague geoportal (www.geoportalpraha.cz, accessed on 10 October 2023) in a raster format with a resolution of 1 m. The models were created via photogrammetry from aerial imagery and updated in 2018.

For statistical analysis, all input data were aggregated into a square grid with a spatial resolution of 30×30 m using the mean (NDVI, LST, BH) and sum (BC) values. The river and lakes variables represented the distance of the center of each square from the nearest lake or from the Vltava river. The distances were calculated using the Near function in GIS. All GIS tasks were handled in ArcGIS Pro 2.7.0. The described data creation process is clearly displayed in Figure 3.

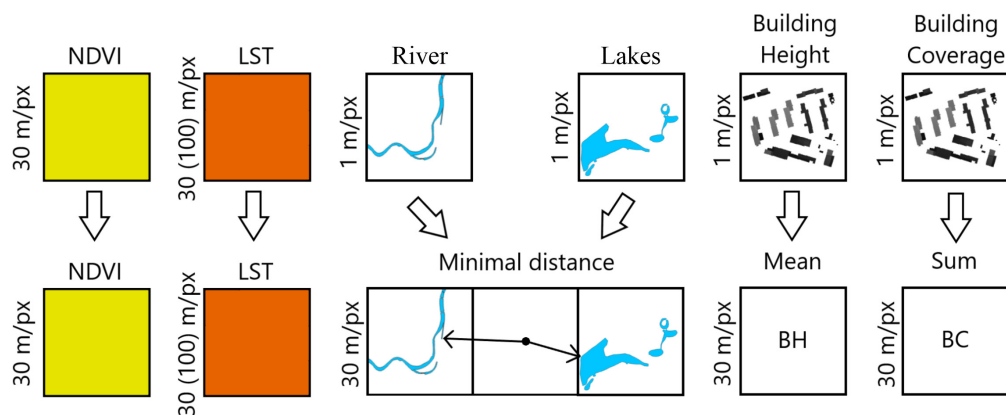


Figure 3. Creating data for statistical analysis. Input data in the upper row were used for preparing data (factors) in the bottom one.

In order to more closely investigate the local effect of blue bodies, we also performed a local statistical analysis focusing on areas around lakes and the river. First, envelope areas of 100, 200, 300, 400, and 500 m around these water bodies were created. The maximum buffer distance was set to 500 m based on the results by Lin et al. [20]. With every 100 m increase, the extent of the area was expanded by approximately 3 pixels in all directions. Subsequently, the Extract by Mask function in the ArcGIS PRO software 2.8.2 was used to crop the raster data. The blue bodies themselves were removed from the data for modeling purposes.

2.4. Statistical Analysis

The relationships between the LST and the five investigated factors—BH, BC, NDVI, distance to river, and distance to large lakes—were assessed using multiple linear regression model techniques. Firstly, an ordinary least square regression model, a common technique for estimating the coefficients of linear regression models, was applied both to the whole of Prague and to each of the three zones separately, yielding a model in the form of $Y = \beta \cdot X$, where Y is a vector of LST, X is the matrix of the five factors, and β is the transposed vector of appropriate regression parameters, $\beta_0, \beta_1, \dots, \beta_5$.

The regression coefficients were calculated to express the effect of the factors on the land surface temperature. Since the regression coefficients do not capture the relative importance of particular predictors, we used complementary methods to gain a deeper

understanding of the resulting model. There are several approaches to the importance measures of particular predictors (e.g., based on standardized coefficients, partial correlation, or commonality analysis). In this study, we utilized the dominance analysis approach outlined by Azen and Budescu [42]. A brief description of the method is as follows: Firstly, all possible submodels with the given set of predictors are determined. The proportion of explained variance which is accounted by the model consisting of different possible predictors combination is measured. The additional contribution of a given predictor is captured by the increase in explained variance that results from adding that predictor to the model. Thus, the additional contributions of a predictor are computed as the increases in the proportion of variance accounted for when the predictor is added to each subset of the remaining predictors. The last stage of analysis summarizes the additional contributions of predictors by averaging all values. The detailed description of the approach is much more complex [42]. The R package `dominanceanalysis` and the function of the same name were employed for practical implementation.

In order to verify the model, some basic indicators of model quality were examined. Firstly, the variance inflation factor (VIF) of the predictors was calculated to rule out multicollinearity (using a threshold of $VIF = 5$). Secondly, residues of the models were tested for normality (Kolmogorov–Smirnov test) and heteroscedasticity (Breusch–Pagan test). In both cases, the null hypotheses were rejected, i.e., the model residuals were shown to suffer from both non-normality and heteroscedasticity. As the spatial autocorrelation of residuals was detected using the global Moran's I, this violation of model assumptions can be attributed to spatial dependency, which is natural for spatial data. The spatial autocorrelation of all the predictors is the cause of the model's non-stationarity.

To avoid autocorrelation and non-stationarity problems and to prove the stability of the principal model, a simulation with randomization (random-sample model) was applied. The regression analysis was repeated one hundred times, each time on a randomly selected sample representing 10% of the input data in each run. Point estimates of the mean values of all variables (regression coefficients, t statistics, relative importance, etc.) were calculated, and the results are presented in Appendix A. The results of the random-sample models are almost identical to the results calculated for the principal models, and, as such, we consider the models to be numerically stable.

3. Results

3.1. City Overview

Preliminary results presenting characteristics and LSTs in the zones of Prague are displayed in Figure 4. Unsurprisingly, BH and BC increase towards the city center, whereas the NDVI decreases. The NDVI, BH, and BC change less between the inner and outer compact city than between the outer compact city and the city's outskirts. In other words, the spatial characteristics of the outskirts differ from those of the compact zones with a higher mutual similarity.

The results clearly show that the mean LST in Prague increases towards the city center. At 4.5 °C, the overall increase is substantial. The LST difference between the city's outskirts and the outer compact city (3.6 °C) is markedly larger than that between the outer and inner compact city (0.9 °C). This indicates a possible relation to both the position of the zone and its spatial characteristics. In addition, the variability of the LST within each zone is relatively low (Figure 4). The mean LST within the individual grid squares on the outskirts ranged from 29.2 °C to 57.6 °C, while in the outer compact city, it ranged from 30.7 °C to 65.0 °C, and in the inner compact city, it ranged from 32.0 °C to 62.7 °C. Standard deviations in all three zones were similar. Such differences in LST reveal the influence of the characteristics within each square grid.

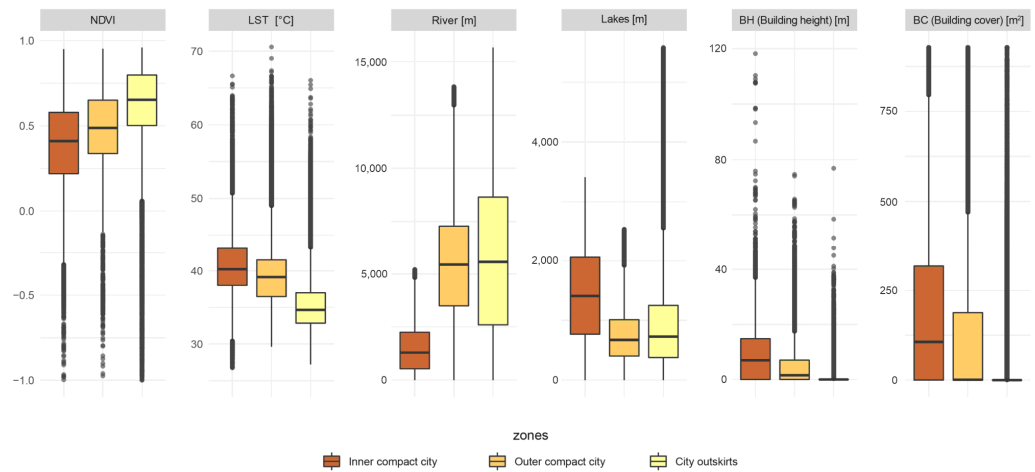


Figure 4. Box plot with characteristics of the three Prague zones indicated in Figure 1.

3.2. Association of LST and Individual Factors in Prague as a Whole (Principal Models)

We examined the mean values of BH, BC, NDVI, proximity to the river, and proximity to lakes through multiple rounds of regression modeling in order to find their relative effects on LST. Regression was calculated from four datasets (data for the whole of Prague and for the three zones separately). The results, expressed as regression coefficients (b) and the relative significance of predictors on the total model variance (R²), are presented in Appendix B. The importance of individual predictors, expressed with their contribution to the total R² in the three zones of Prague, is displayed in Figure 5. The results show that the combination of all examined factors can explain between 62.1 (inner compact city) and 73.2 (outer compact city) percent of the total LST variability in Prague (see the total model variance R²). In all four regression models, all the input predictors were marked as statistically significant at the level of $\alpha = 0.01$.

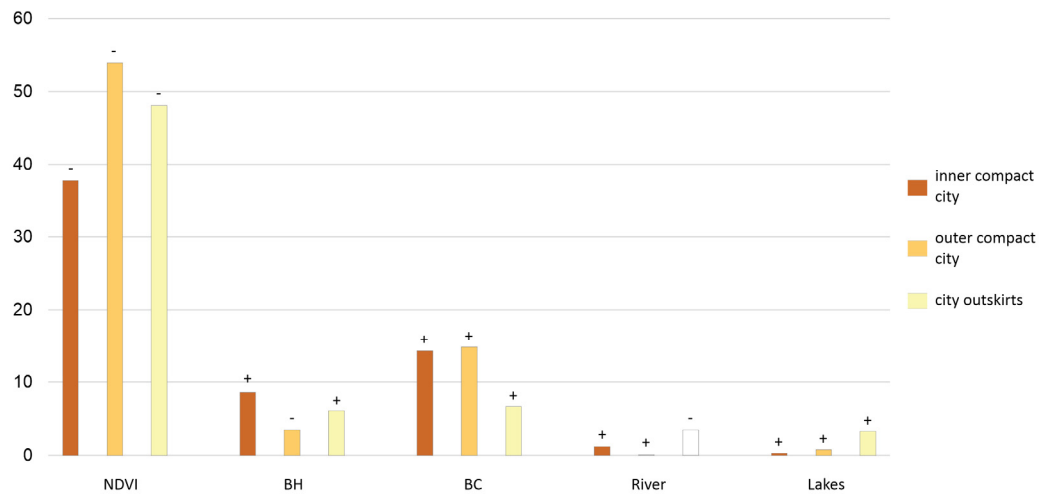


Figure 5. The relative effect (R²) of the examined factors on LST in the inner compact city, outer compact city, and city outskirts. The ± values represent positive effect or negative effect (i.e., reduction of LST). The ± values correspond to ± values of “b” in the tables in Appendices A–D. The only outline colors indicate values with no or only borderline statistical significance.

In all zones, the NDVI showed the most decisive relative influence on LST variation when compared to other factors (clearly visible in Figure 5). The NDVI alone explains most of the LST variability in Prague (37.7–53.9%); the NDVI’s influence was strongest in the outer compact city and weakest in the inner compact city, which has the lowest greenery and highest building density. BC was the second most influential factor; the impact of the other factors on the LST is less unambiguous. The NDVI vs. LST regression coefficient is negative, with

absolute values between -10.3 and -14.9 . It can be interpreted as follows: an increase in NDVI in Prague from 0 (i.e., theoretically no vegetation) to 1 (i.e., the theoretical maximum vegetation cover) leads to a temperature decrease of 10.3 – 14.9 °C. Analogically, if the built-up area within a grid square increases by 1 m^2 , the LST in this square increases by 0.004 °C.

The overall relative impact of the horizontal BC was higher than that of the vertical BH in all zones, even if the ranking of the factors' importance differs slightly among city zones. The influence of BC is high in the compact city (both inner and outer); it decreases in the city's outskirts with low-density housing, where its influence is almost identical to BH. The influence of BH is lowest in the outer compact city, with low-rise buildings, and is highest in the inner compact city, with a block structure of mostly four-to-six-storey buildings. As we expected, the effect of the river and lakes variables was the weakest of all the factors analysed.

The NDVI had a definite cooling effect, while BC caused a definite warming effect. The rest of the factors exhibited some level of heterogeneity. The effect of BH was warming, except for in the outer compact city, where it had a slight cooling effect. In most cases, blue bodies had only a negligible effect on the LST, and the cooling effect further dropped with increasing distance from water bodies. Nevertheless, some heterogeneity in the blue bodies' effects was manifested in the city's outskirts, where the river had a (negligible) warming effect, whereas the cooling effect of the lakes increased. Therefore, the effect of blue bodies was further locally investigated only in the vicinity of a maximum distance of 500 m from the blue bodies.

3.3. Association of LST and Individual Factors around the River and Lakes

The multiple regression models were calculated for a maximum of 500 m from the river and lakes in 100 m intervals. The results are presented in the tables in Appendices C and D. The relative significance of the individual factors (R^2) is displayed in Figure 6; Figure 6a represents the distance from the lakes, and Figure 6b represents the distance from the river. Where this local approach could be employed, the models explained a higher percentage of variability than the principal model. Regardless of the zones, the model explained approximately 72% of the variability in the vicinity of lakes and 77–78% of the variability in the vicinity of the river. The percentage varies slightly between zones, being highest in the outer compact city (78.7% in the case of lakes, 82.3% in the case of the river).

The River is the second most influential factor within 200 m of its surroundings (Figure 6b). It is also evident that its influence decreases with the analysed range (100–500 m). It does not decrease equally in all three zones; it drops much more steeply in the outer compact city than in the remaining zones. It must, however, be mentioned that the outer compact city is in direct contact with the river only in a very small area. As such, the area within 100 m of the river is very small, while within 200–500 m of the river, greater and more diverse areas of the outer compact city are included. In effect, the data describing the outer compact city within 100 m of the river and at greater distances differ in the character of the area and the rapid drop; therefore, the data should not be used to draw hasty conclusions. The most gradual decline can be seen in the city's outskirts, where the air can flow without being blocked by buildings. On the other hand, the influence of lakes was low even in their closest vicinity and further decreased with distance. Still, where the effect was observed, it was always a cooling effect (LST increased with distance).

In addition, the model confirms the constant and significant cooling effect of the NDVI throughout various areas of Prague. A relatively lower effect of the NDVI can be seen around the lakes in the inner compact city. Conversely, the NDVI is a more powerful factor around lakes than around the river in the outer compact city, where vast parks surround the lakes. The significant and relatively stable positive effect is also confirmed in the case of BC, while the effect of BH remains heterogeneous only in the outer compact city. Lastly, the effect of the river appears to be slightly warming at more than 500 m from the river in the

outer compact city and on the outskirts. This effect is probably associated with some other, non-analysed factor.

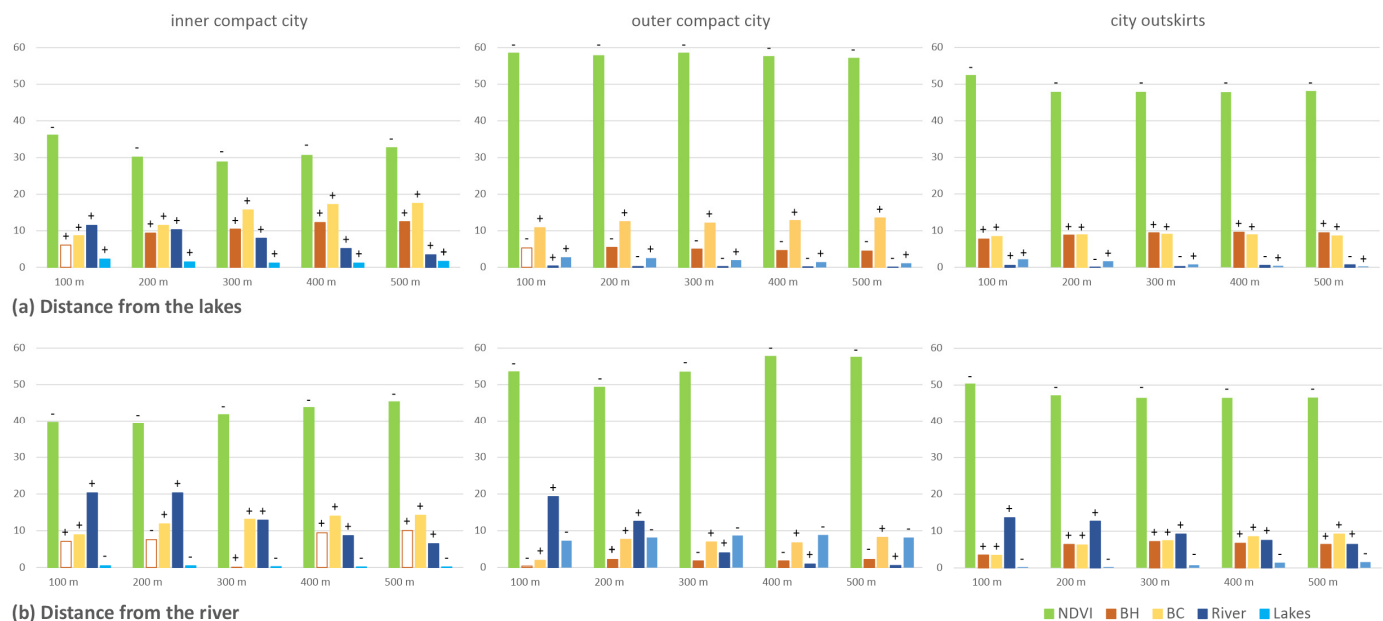


Figure 6. The relative effect (R^2) of the examined factors on LST from lakes (a) and the river (b) at distances of 100, 200, 300, 400, and 500 m, respectively. The \pm values represent positive effect or negative effect (i.e., reduction of LST). The only outline colors indicate values with no or only borderline statistical significance.

4. Discussion

4.1. Comparing the Effect of the Green and Blue Bodies on LST

In line with previous research [33,43], our results confirmed the substantial cooling effect of green bodies on summer days in a temperate climate. In addition, we found that the NDVI effect clearly outweighs all other factors, and it slightly differs between the city zones. It is lowest in the inner compact city and higher in zones with a low-rise city structure with trees. This has two implications. Firstly, the efficiency of the cooling effect increases with the size and density of green bodies [2,15,17]. Our results show large semi-dense green bodies to have the highest cooling effect in Prague, adding that the connectivity of greenery may be another supporting factor of the cooling effectiveness and, at the same time, bring additional ecological benefits [44]. Secondly, the efficiency of the cooling effect is greater in lower densities compared to mid-rise city structures. This can be explained by the fact that taller buildings already provide cooling shade [13,32], making tree shade less effective.

4.2. Comparing the Effect of the Lakes and the River on LST

Our results confirmed the local cooling effect [18,20] of the river but not of the lakes. The cooling effect of the river was more effective in the compact city of Prague, where it was about half of that of the NDVI. In compact northern Chinese cities, the effect of rivers even exceeded the influence of green bodies [28]. We believe we can explain this inconsistency with the fact that greenery is simply more effective in a drier climate, such as that of Central Europe [3], because the evaporative cooling of greenery is reduced by high air humidity [45]. Humidity might be higher locally around water bodies, and thus may reduce the cooling effect of greenery. However, we cannot confirm this in this study (having not measured the humidity). Nevertheless, the NDVI effect is not lower around the water bodies than elsewhere in Prague.

Our results show the strong influence of the river in adjacent areas within an envelope of 100 m in the entire compact city. With a distance increase of another 100 m, the influence

remains strong in the inner compact city but sharply drops in the outer compact city. The difference in elevation between the river and its banks (elevation difference) may likely play a role [1]. In another study, increasing elevation (relative height to sea level) was found to be a non-negligible factor leading to LST reduction [43]. However, in this case, the elevation difference is not big enough (approx. 4 m) to cause such a drop. Instead, the urban morphology seems to matter. In the outer compact city, there is a short strip of compact buildings within 100 m of the river in the north (corresponding to those in the inner compact city), and there are low-rise buildings within 200–500 m of the river in the south (corresponding to those on the city's outskirts). The results imply that the effective river cooling distance, if not considering the wind speed, greatly depends on the type of urban morphology around the river, and that the cooling distance is more extensive within the compact urban morphology than within low-rise buildings.

The negligible effect of lakes was, similar to our study, also found in other European cities, such as Augsburg, Germany [27], and several Dutch cities [19]. Here, the wind speed, which, according to some recent studies [45,46], significantly mitigates the SUHI, was rather low (Augsburg: $2\text{--}7\text{ ms}^{-1}$; Netherlands: 2.8 ms^{-1}). In Prague, one meteorological station measured a similar wind speed (8 ms^{-1}). Although air mass and circulation can be locally differentiated across Prague, we do not expect the differences to be large. Therefore, we confirm the negligible effect of blue bodies sized between 0.1 ha and 35.8 ha (mean: 1.5 ha, std.: 3.6 ha) in rather light wind conditions. The effect might be more significant if the wind is stronger, the lakes are larger, or the assessed distance is smaller. For instance, Wang and Ouyang [18] assessed only lakes larger than 3 ha; Lin et al. [20] found lakes' effective cooling distance to be only 40–70 m. However, it is insufficient to consider only larger lakes for planning purposes in a European context, and, inversely, the shorter distance is unnecessarily detailed considering the fact that the usual building block size in Prague is approx. 100 m.

4.3. Explaining Urban Morphology

Consistent with other studies [1,27], our findings show that in the city, BC is a predominant factor generating a warming effect; we found that the warming effect increases with city compactness. The same principle was also found in the subtropical monsoon climate of the city of Nanjing in China [2]. In Prague, while the BC has a similar effect (14%) across the compact city (with the character of LCZ 2, 5, 6), it drops by half (to 7%) in low-rise urban morphology on the outskirts (predominantly LCZ 6). On the city's outskirts, where the median built-up area is approx. 20 percent (median BC/ $30 \times 30\text{ m}$) and the median BH is 7.0 m, the warming effects of BC and BH are almost identical. Our results confirmed the heterogeneity of the warming effects of BH in European cities [21]. It was positive in the inner city and on the city's outskirts, but negative in the outer compact city, the city zone with the highest BH variability (BH: 11.5 m; SD: 7.5 m). High-rise buildings were found to reduce LST in Asian cities, such as Beijing [29], Guangzhou [12], and Shanghai [1,31]. The higher BH also provides opportunities for higher BH variability (e.g., BH in Beijing: 16.79 m; SD: 12.7 m [29]), which was suggested as another factor influencing LST [47]. It indicates that the higher buildings increase their cooling effect, providing shade to surrounding low-rise buildings.

4.4. Study Limitations and Further Research

The principal model may contain some inaccuracies due to the spatial effects. To avoid these effects, we designed an independent regression model for every record of the sample solely on the basis of adjacent units, using the structure of residuals (spatial error model) developed by Anselin [48,49] and the approach of geographically weighted regression presented by Brunson et al. [50,51]. Unfortunately, after testing these methods, none of them were suitable due to the large number of records and the consequent computational impracticability. For this reason, we ultimately applied a simulation with randomization, thus partially avoiding the spatial effects. Such a verification confirmed the results and

proved that the outputs are valid and the influence of spatial dependence does not play any substantial role.

The explained variance of the presented models reaches up to 82% (river vicinity), which is comparable with other European studies ranging from 51% to 76% (using four variables, excluding blue bodies) [33] to 85% (using land use characteristics, including sealed surfaces) [27]. The percentage could be increased by including variables such as sealed surfaces (even if they were indirectly and reversely manifested in the NDVI) [2], the elevation and slope of terrain [1,43], local dynamics of wind speed and air humidity [4,46], or sky factors [47].

We discovered the effect of the assessed factors on the three zones of Prague defined for planning purposes. Nevertheless, these zones do not fully correspond with the morphology of the city. Therefore, further research may focus on the influence of the factors on local climate zones [52], which better reflect the morphology and are currently widely used [17], to allow for a broader comparison of results.

The effects of both green and water bodies possess a seasonal variety [18]. The extensive cooling effect we measured in summer will be reduced in autumn and winter once the metabolic activity of the trees is reduced and the leaves wither and fall off [43]. We measured the effects only during the hottest season, when the importance of cooling effects is the greatest [4,15]. Further studies may also focus on green and blue bodies' effects during the spring season, when higher temperatures become more frequent [36], and in late summer, when lawns often become parched.

5. Conclusions

This paper compares and characterizes the effects of green and blue bodies and building height and coverage on land surface temperature in three zones of Prague, Czech Republic. Our findings lead to the conclusion that green and blue bodies and building height and coverage jointly and significantly affect land surface temperature, with the effect of green bodies being by far the most powerful. Because of the local effect of blue bodies, the same comparison was repeated within a 500 m distance of lakes and the Vltava river. A considerable local cooling effect of the river variable was observed, especially within 200 m of the river; however, the effect of the lakes was negligible even within a 100 m distance of the lakes. The considerably notable finding was that the effects of green bodies clearly outweigh those of blue bodies.

Several planning implications can be derived from the presented results. The most evident implication is that the urban adaptation strategies in compact cities in a temperate climate should be based on maximizing live and dense green bodies in compact cities in a temperate climate rather than on forming artificial blue bodies of a lake character.

The local cooling effect of the river was most effective in the compact city, where it reached about half of the effect of the NDVI. The effective cooling distance was 200 m in the compact city. The planning consequence is that alternative measures could be applied within the envelope of 200 m around rivers. Here, the urban structure should be proposed with particular regard to alleviating the river cooling distance.

In the city outskirts, the warming effects of building coverage and height are similar. The planning consequence is that the intensity of greenery should be required to compensate for both building coverage and building height in the city outskirts. This will indirectly hamper vertical development and the resulting developments will better fit the character of the low-rise city structure.

Building coverage is a predominant factor in the city, generating a warming effect, and the warming effect increases with city compactness. As a planning consequence, we suggest adopting planning regulations that would require compensating built-up areas with the intensity of greenery in compact cities. Thus, indirectly, the regulation will promote the vertical development and compactness of cities.

Author Contributions: All authors contributed to the study conception and design. Material preparation, data collection, and analysis were performed by V.K., D.M. and K.M. The first draft of the manuscript was written by V.K. All authors have read and agreed to the published version of the manuscript.

Funding: This research received no external funding.

Data Availability Statement: The data of digital elevation model for Prague presented in this study are openly available on Open data Praha [<https://opendata.praha.eu>, accessed on 10 October 2023]. The satellite data used in this study (temperature, bands for NDVI) are openly available on USGS [<https://earthexplorer.usgs.gov/>, accessed on 10 October 2023].

Acknowledgments: Thanks to Jarek Janošek and Tomáš Peltan for their comments on the manuscript.

Conflicts of Interest: The authors declare no conflicts of interest.

Appendix A

RANDOM SAMPLES MODEL																
	Prague - total				Prague - inner compact city				Prague - outer compact city				Prague - city outskirts			
	b	t	p-value*	relative R ²	b	t	p-value*	relative R ²	b	t	p-value*	relative R ²	b	t	p-value*	relative R ²
Intercept	43.712	956.5	100%		42.81	440.2	100%		45.957	537.4	100%		41.239	743.3	100%	
NDVI	-12.771	-231.5	100%	45.7%	-10.377	-80.8	100%	37.9%	-14.946	-157.1	100%	53.8%	-10.773	-163.2	100%	48.2%
BH	0.0476	20.3	100%	8.6%	0.03744	9.2	100%	8.6%	-0.019699	-6.6	100%	3.5%	0.1543	19.5	100%	6.1%
BC	0.00571	60.4	100%	14.7%	0.004209	25.2	100%	14.2%	0.004757	38.1	100%	14.8%	0.004284	19.0	100%	6.8%
River	-0.000023	-6.7	100%	0.6%	0.000545	22.1	100%	1.2%	0.000016	2.4	64%	0.2%	-0.000008	-2.3	63%	0.1%
Lakes	0.000296	18.7	100%	1.2%	0.000128	3.7	99%	0.3%	0.000334	8.5	100%	0.8%	0.000584	34.4	100%	3.4%
sample size																
F statistics	23 136				29 331				89 340				83 735			
R ²	0.7087				0.6223				0.7314				0.6436			

* indicates, in how many of the randomly created models the predictor has been significant at the level alpha = 0.05

Appendix B

PRINCIPAL MODEL																
	Prague - total				Prague - inner compact city				Prague - outer compact city				Prague - city outskirts			
	b	t	p-value	relative R ²	b	t	p-value	relative R ²	b	t	p-value	relative R ²	b	t	p-value	relative R ²
Intercept	43.71	3027.7	< 2 x 10 ⁻¹⁶		42.78	1327.1	< 2 x 10 ⁻¹⁶		45.96	1700.1	< 2 x 10 ⁻¹⁶		41.22	2351.5	< 2 x 10 ⁻¹⁶	
NDVI	-12.77	-732.9	< 2 x 10 ⁻¹⁶	45.7%	-10.33	-242.9	< 2 x 10 ⁻¹⁶	37.7%	-14.95	-497.2	< 2 x 10 ⁻¹⁶	53.9%	-10.75	-515.5	< 2 x 10 ⁻¹⁶	48.1%
BH	0.0478	64.5	< 2 x 10 ⁻¹⁶	8.6%	0.03807	28.3	< 2 x 10 ⁻¹⁶	8.6%	-0.01934	-20.4	< 2 x 10 ⁻¹⁶	3.5%	0.1529	61.2	< 2 x 10 ⁻¹⁶	6.1%
BC	0.00571	191.1	< 2 x 10 ⁻¹⁶	14.7%	0.004224	76.2	< 2 x 10 ⁻¹⁶	14.3%	0.004713	119.4	< 2 x 10 ⁻¹⁶	14.8%	0.004349	61.1	< 2 x 10 ⁻¹⁶	6.7%
River	-0.000023	-21.1	< 2 x 10 ⁻¹⁶	0.6%	0.000546	66.7	< 2 x 10 ⁻¹⁶	1.2%	0.000016	7.4	1.33 x 10 ⁻¹³	0.2%	-0.000008	-6.8	9.16 x 10 ⁻¹²	0.1%
Lakes	0.000296	59.4	< 2 x 10 ⁻¹⁶	1.2%	0.000125	11.1	< 2 x 10 ⁻¹⁶	0.3%	0.000347	27.6	< 2 x 10 ⁻¹⁶	0.8%	0.000584	108.7	< 2 x 10 ⁻¹⁶	3.3%
sample size	475 898				80 886				163 783				231 229			
F statistics	23 160				26 510				89 180				83 500			
R ²	0.7087				0.6211				0.7314				0.6436			

Appendix C

MODEL CALCULATED IN DISTANCES FROM THE RIVER																				
INNER COMPACT CITY																				
	100m				200m				300m				400m				500m			
	b	t	p-value	relative R ²	b	t	p-value	relative R ²	b	t	p-value	relative R ²	b	t	p-value	relative R ²	b	t	p-value	relative R ²
Intercept	40.42	328.0	< 2 x 10 ⁻¹⁶		41.58	393.5	< 2 x 10 ⁻¹⁶		42.55	456.5	< 2 x 10 ⁻¹⁶		43.28	521.9	< 2 x 10 ⁻¹⁶		43.79	589.9	< 2 x 10 ⁻¹⁶	
NDVI	-12.12	-71.4	< 2 x 10 ⁻¹⁶	39.7%	-13.12	-94.3	< 2 x 10 ⁻¹⁶	39.3%	-13.88	-113.2	< 2 x 10 ⁻¹⁶	41.8%	-14.22	-129.9	< 2 x 10 ⁻¹⁶	43.8%	-14.48	-147.3	< 2 x 10 ⁻¹⁶	45.3%
BH	0.005938	1.1	0.275	7.1%	-0.005547	-1.4	0.166	7.6%	0.0041	1.2	0.0244	0.1%	0.0057	1.9	0.062	9.5%	0.00677	2.4	0.0161	10.1%
BC	0.001288	5.5	5.17 x 10 ⁻⁹	8.9%	0.002503	14.8	< 2 x 10 ⁻¹⁶	11.9%	0.00244	17.2	< 2 x 10 ⁻¹⁶	13.1%	0.00246	20.1	< 2 x 10 ⁻¹⁶	14.0%	0.00246	22.5	< 2 x 10 ⁻¹⁶	14.2%
River	0.0689	53.0	< 2 x 10 ⁻¹⁶	20.3%	0.03347	69.9	< 2 x 10 ⁻¹⁶	20.3%	0.01877	69.7	< 2 x 10 ⁻¹⁶	12.9%	0.0116	66.1	< 2 x 10 ⁻¹⁶	8.7%	0.00836	66.0	< 2 x 10 ⁻¹⁶	6.5%
Lakes	-0.000182	-3.9	9.32 x 10 ⁻⁵	0.5%	-0.000125	-3.3	0.00084	0.5%	-0.000065	-2.0	0.045	0.3%	-0.000577	-2.1	0.0376	0.2%	-0.000067	-2.7	0.0066	0.2%
sample size	3 624				6 603				9 702				12 791				15 817			
F statistics	2 352				4 710				6 422				8 159				10 180			
R ²	76.4%				78.1%				76.8%				78.1%				76.3%			
OUTER COMPACT CITY																				
	100m				200m				300m				400m				500m			
	b	t	p-value	relative R ²	b	t	p-value	relative R ²	b	t	p-value	relative R ²	b	t	p-value	relative R ²	b	t	p-value	relative R ²
Intercept	44.96	76.9	< 2 x 10 ⁻¹⁶		43.26	137.1	< 2 x 10 ⁻¹⁶		44.85	198.9	< 2 x 10 ⁻¹⁶		45.37	298.7	< 2 x 10 ⁻¹⁶		45.57	391.5	< 2 x 10 ⁻¹⁶	
NDVI	-11.98	-26.8	< 2 x 10 ⁻¹⁶	53.5%	-12.41	-42.0	< 2 x 10 ⁻¹⁶	49.3%	-12.56	-53.8	< 2 x 10 ⁻¹⁶	53.4%	-12.62	-72.3	< 2 x 10 ⁻¹⁶	57.7%	-12.64	-85.2	< 2 x 10 ⁻¹⁶	57.5%
BH	-0.086	-2.9	0.0045	0.4%	-0.074	-4.9	1.19 x 10 ⁻⁵	2.2%	-0.0509	-5.0	7.35 x 10 ⁻⁷	1.8%	-0.0322	-4.2	2.92 x 10 ⁻⁵	1.8%	-0.03334	-5.5	3.64 x 10 ⁻⁶	2.2%
BC	0.00247	3.0	0.0031	2.0%	0.00326	7.0	5.86 x 10 ⁻¹²	7.7%	0.00245	7.4	1.79 x 10 ⁻¹³	7.0%	0.00214	8.3	< 2 x 10 ⁻¹⁶	6.7%	0.00234	10.9	< 2 x 10 ⁻¹⁶	8.2%
River	0.03505	11.6	< 2 x 10 ⁻¹⁶	19.3%	0.0215	17.6	< 2 x 10 ⁻¹⁶	12.6%	0.00728	11.4	< 2 x 10 ⁻¹⁶	40.0%	0.0031	8.7	< 2 x 10 ⁻¹⁶	1.0%	0.00108	4.8	2.05 x 10 ⁻⁶	0.6%
Lakes	-0.00264	-8.3	4.52 x 10 ⁻¹⁵	7.3%	-0.000986	-5.9	4.54 x 10 ⁻⁹	8.2%	-0.00125	-10.0	< 2 x 10 ⁻¹⁶	8.7%	-0.001235	-13.4	< 2 x 10 ⁻¹⁶	8.9%	-0.00109	-15.3	< 2e-16	8.2%
sample size	297				830				1 614				2 260				3 834			
F statistics	276				657				961				1 694				2 510			
R ²	82.3%				79.8%				74.9%				76.1%				76.6%			
CITY OUTSKIRTS																				
	100m				200m				300m				400m				500m			
	b	t	p-value	relative R ²	b	t	p-value	relative R ²	b	t	p-value	relative R ²	b	t	p-value	relative R ²	b	t	p-value	relative R ²
Intercept	40.29	373.2	< 2 x 10 ⁻¹⁶		40.81	921.6	< 2 x 10 ⁻¹⁶		41.46	552.6	< 2 x 10 ⁻¹⁶		41.86	1142.9	< 2 x 10 ⁻¹⁶		42.05	671.4	< 2 x 10 ⁻¹⁶	
NDVI	-11.56	-80.2	< 2 x 10 ⁻¹⁶	50.4%	-11.58	-225.1	< 2 x 10 ⁻¹⁶	47.2%	-11.83	-114.8	< 2 x 10 ⁻¹⁶	46.5%	-11.92	-255.0	< 2 x 10 ⁻¹⁶	46.5%	-11.82	-133.7	< 2 x 10 ⁻¹⁶	46.6%
BH	0.04659	3.4	0.00075	3.5%	0.1206	17.9	< 2 x 10 ⁻¹⁶	6.4%	0.136	14.9	< 2 x 10 ⁻¹⁶	7.2%	0.1069	38.4	< 2 x 10 ⁻¹⁶	6.7%	0.09984	14.9	< 2 x 10 ⁻¹⁶	6.4%
BC	0.00149	3.4	0.00068	3.4%	0.001809	31.4	3.03 x 10 ⁻¹³	6.2%	0.002261	11.0	< 2 x 10 ⁻¹⁶	7.4%	0.003577	21.8	< 2 x 10 ⁻¹⁶	8.5%	0.004225	24.5	< 2 x 10 ⁻¹⁶	9.2%
River	0.04109	40.4	< 2 x 10 ⁻¹⁶	13.6%	0.02075	-16.9	< 2 x 10 ⁻¹⁶	12.7%	0.0123	52.1	< 2 x 10 ⁻¹⁶	9.2%	0.008535	-16.6	< 2 x 10 ⁻¹⁶	7.5%	0.00616	51.1	< 2 x 10 ⁻¹⁶	6.4%
Lakes	-0.000371	-8.7	< 2 x 10 ⁻¹⁶	0.3%	-0.000357	34.3	< 2 x 10 ⁻¹⁶	0.3%	-0.000437	-14.0	< 2 x 10 ⁻¹⁶	0.7%	-0.000483	11.5	< 2 x 10 ⁻¹⁶	1.4%	-0.000481	-17.8	< 2 x 10 ⁻¹⁶	1.6%
sample size	3 994				7 239				9 932				12 352				14 623			
F statistics	1 969				3 858				4 881				5 915				6 863			
R ²	71.1%				72.7%				71.1%				70.7%				70.1%			

no statistical significance
on the border of statistical significance

Appendix D

MODEL CALCULATED IN DISTANCES FROM THE LAKES																				
INNER COMPACT CITY																				
	100m				200m				300m				400m				500m			
	b	t	p-value	relative R ²	b	t	p-value	relative R ²	b	t	p-value	relative R ²	b	t	p-value	relative R ²	b	t	p-value	relative R ²
Intercept	39.04	148.6	< 2 × 10 ⁻¹⁶		38.67	231.4	< 2 × 10 ⁻¹⁶		39.07	1171.5	< 2 × 10 ⁻¹⁶		39.59	390.8	< 2 × 10 ⁻¹⁶		40.14	455.8	< 2 × 10 ⁻¹⁶	
NDVI	-8.027	-25.2	< 2 × 10 ⁻¹⁶	36.1%	-7.06	-37.4	< 2 × 10 ⁻¹⁶	30.1%	-7.003	-286.2	< 2 × 10 ⁻¹⁶	28.8%	-7.577	-65.1	< 2 × 10 ⁻¹⁶	30.6%	-8.298	-80.6	< 2 × 10 ⁻¹⁶	32.7%
BH	0.0175	0.93	0.353	6.1%	0.0437	4.05	5.32 × 10 ⁻⁵	9.4%	0.0543	28.9	< 2 × 10 ⁻¹⁶	10.5%	0.0652	12.5	< 2 × 10 ⁻¹⁶	12.3%	0.0672	15.8	< 2 × 10 ⁻¹⁶	12.5%
BC	0.00416	5.8	8 × 10 ⁻⁹	8.7%	0.00489	11.9	< 2 × 10 ⁻¹⁶	11.5%	0.00525	49.9	< 2 × 10 ⁻¹⁶	15.7%	0.00520	26.9	< 2 × 10 ⁻¹⁶	17.2%	0.00501	31.7	< 2 × 10 ⁻¹⁶	17.5%
River	0.00121	16.4	< 2 × 10 ⁻¹⁶	11.5%	0.00114	25	< 2 × 10 ⁻¹⁶	10.3%	0.000952	-20.7	1.33 × 10 ⁻¹³	8.0%	0.00078	33.3	< 2 × 10 ⁻¹⁶	5.2%	0.000664	34.7	< 2 × 10 ⁻¹⁶	3.5%
Lakes	0.0104	3.6	0.0034	2.3%	0.00522	5.7	1.59 × 10 ⁻⁸	1.5%	0.00239	32	< 2 × 10 ⁻¹⁶	1.2%	0.00219	8.2	2.6 × 10 ⁻¹⁶	1.2%	0.00219	11.9	< 2 × 10 ⁻¹⁶	1.7%
sample size	770				2269				4576				7304				10306			
F statistics	280				764				1642				2916				4367			
R ²	64.5%				62.7%				64.2%				66.6%				67.9%			
OUTER COMPACT CITY																				
	100m				200m				300m				400m				500m			
	b	t	p-value	relative R ²	b	t	p-value	relative R ²	b	t	p-value	relative R ²	b	t	p-value	relative R ²	b	t	p-value	relative R ²
Intercept	44.54	365.4	< 2 × 10 ⁻¹⁶		45.14	583.1	< 2 × 10 ⁻¹⁶		45.57	755.6	< 2 × 10 ⁻¹⁶		45.94	915.8	< 2 × 10 ⁻¹⁶		46.11	1057.6	< 2 × 10 ⁻¹⁶	
NDVI	-12.61	-93.7	< 2 × 10 ⁻¹⁶	58.5%	-13.49	-160.3	< 2 × 10 ⁻¹⁶	57.8%	-14.04	-214.3	< 2 × 10 ⁻¹⁶	57.5%	-14.58	-266.3	< 2 × 10 ⁻¹⁶	57.6%	-14.88	-310.1	< 2 × 10 ⁻¹⁶	57.1%
BH	-0.01003	-1.86	0.063	5.3%	-0.0131	-4.3	1.25 × 10 ⁻⁵	5.5%	-0.00812	-3.6	0.00032	5.0%	-0.0139	-7.8	4.5 × 10 ⁻⁵	4.6%	-0.0171	-11.4	< 2 × 10 ⁻¹⁶	4.5%
BC	0.001167	5.25	1.56 × 10 ⁻⁷	10.9%	0.00226	17.8	< 2 × 10 ⁻¹⁶	12.5%	0.002423	25.6	< 2 × 10 ⁻¹⁶	12.1%	0.00279	36.4	< 2 × 10 ⁻¹⁶	12.8%	0.00318	48.9	< 2 × 10 ⁻¹⁶	13.5%
River	-0.000114	-11.6	< 2 × 10 ⁻¹⁶	0.4%	-0.000102	-16.6	< 2 × 10 ⁻¹⁶	0.3%	-0.000094	-20	< 2 × 10 ⁻¹⁶	0.3%	-0.000084	-21.7	< 2 × 10 ⁻¹⁶	0.2%	-0.000066	-19.9	< 2 × 10 ⁻¹⁶	0.1%
Lakes	0.0112	12.3	< 2 × 10 ⁻¹⁶	2.8%	0.0061	20.9	< 2 × 10 ⁻¹⁶	2.6%	0.00379	24.6	< 2 × 10 ⁻¹⁶	2.0%	0.00263	26.8	< 2 × 10 ⁻¹⁶	1.5%	0.00182	26.5	< 2 × 10 ⁻¹⁶	1.2%
sample size	4186				12395				23680				37065				51866			
F statistics	2947				9132				15810				24370				33490			
R ²	77.9%				78.7%				76.9%				76.7%				76.4%			
CITY OUTSKIRTS																				
	100m				200m				300m				400m				500m			
	b	t	p-value	relative R ²	b	t	p-value	relative R ²	b	t	p-value	relative R ²	b	t	p-value	relative R ²	b	t	p-value	relative R ²
Intercept	42.08	625.6	< 2 × 10 ⁻¹⁶		41.78	921.6	< 2 × 10 ⁻¹⁶		41.58	939.6	< 2 × 10 ⁻¹⁶		41.76	1142.9	< 2 × 10 ⁻¹⁶		41.87	1327.4	< 2 × 10 ⁻¹⁶	
NDVI	-11.59	-146.8	< 2 × 10 ⁻¹⁶	52.5%	-11.22	-225.1	< 2 × 10 ⁻¹⁶	50.5%	-10.6	-212.9	< 2 × 10 ⁻¹⁶	47.9%	-10.55	-255	< 2 × 10 ⁻¹⁶	47.8%	-10.53	-293.6	< 2 × 10 ⁻¹⁶	48.1%
BH	0.0546	7.1	1.04 × 10 ⁻¹¹	7.7%	0.1039	17.9	< 2 × 10 ⁻¹⁶	8.8%	0.1425	29.4	< 2 × 10 ⁻¹⁶	9.4%	0.1606	38.4	< 2 × 10 ⁻¹⁶	9.6%	0.169	45.9	< 2 × 10 ⁻¹⁶	9.4%
BC	0.00171	11.2	5.12 × 10 ⁻¹²	8.4%	0.002243	31.4	< 2 × 10 ⁻¹⁶	8.9%	0.00256	18.4	< 2 × 10 ⁻¹⁶	9.0%	0.002538	21.8	< 2 × 10 ⁻¹⁶	8.9%	0.002497	24.7	< 2 × 10 ⁻¹⁶	8.6%
River	-0.000045	-19.5	< 2 × 10 ⁻¹⁶	0.5%	-0.000013	-16.9	< 2 × 10 ⁻¹⁶	0.1%	-0.000019	-7.6	2.81 × 10 ⁻¹⁴	0.2%	-0.000034	-16.6	< 2 × 10 ⁻¹⁶	0.5%	-0.000041	-23.3	< 2 × 10 ⁻¹⁶	0.7%
Lakes	0.0141	24.6	< 2 × 10 ⁻¹⁶	2.2%	0.00519	34.3	< 2 × 10 ⁻¹⁶	1.7%	0.00192	17.9	< 2 × 10 ⁻¹⁶	0.8%	0.000780	11.5	< 2 × 10 ⁻¹⁶	0.4%	0.000231	4.8	1.36 × 10 ⁻⁶	0.3%
sample size	9791				23058				38794				55692				72951			
F statistics	4849				10740				15990				22850				29830			
R ²	71.2%				70.0%				67.3%				67.2%				67.2%			
no statistical significance																				

References

- Sun, F.; Liu, M.; Wang, Y.; Wang, H.; Che, Y. The Effects of 3D Architectural Patterns on the Urban Surface Temperature at a Neighborhood Scale: Relative Contributions and Marginal Effects. *J. Clean. Prod.* **2020**, *258*, 120706. [CrossRef]
- Zhou, L.; Yuan, B.; Hu, F.; Wei, C.; Dang, X.; Sun, D. Understanding the Effects of 2D/3D Urban Morphology on Land Surface Temperature Based on Local Climate Zones. *Build. Environ.* **2022**, *208*, 108578. [CrossRef]
- Manoli, G.; Fatichi, S.; Schlöpfer, M.; Yu, K.; Crowther, T.W.; Meili, N.; Burlando, P.; Katul, G.G.; Bou-Zeid, E. Magnitude of Urban Heat Islands Largely Explained by Climate and Population. *Nature* **2019**, *573*, 55–60. [CrossRef]
- Gunawardena, K.R.; Wells, M.J.; Kershaw, T. Utilising Green and Bluespace to Mitigate Urban Heat Island Intensity. *Sci. Total Environ.* **2017**, *584–585*, 1040–1055. [CrossRef]
- Bay, J.H.P.; Lehmann, S. *Growing Compact: Urban Form, Density and Sustainability*; Bay, J.H.P., Lehmann, S., Eds.; Routledge: Oxon, NY, USA, 2017.
- EC (European Commission). *Green Paper: Towards a New Culture for Urban Mobility*; Office for the Official Publications of the European Communities: Luxembourg, 2007.
- Assessment, A.C. *Compact City Policies*; OECD Publishing: Paris, France, 2012; ISBN 9789264167865.
- Urban, A.; Fonseca-Rodríguez, O.; Di Napoli, C.; Plavcová, E. Temporal Changes of Heat-Attributable Mortality in Prague, Czech Republic, over 1982–2019. *Urban Clim.* **2022**, *44*, 101197. [CrossRef]
- Ayanlade, A. Remote Sensing Approaches for Land Use and Land Surface Temperature Assessment: A Review of Methods. *Int. J. Image Data Fusion* **2017**, *8*, 188–210. [CrossRef]
- Gemitzi, A.; Dalampakis, P.; Falalakis, G. Detecting Geothermal Anomalies Using Landsat 8 Thermal Infrared Remotely Sensed Data. *Int. J. Appl. Earth Obs. Geoinf.* **2021**, *96*, 102283. [CrossRef]
- Wang, Y.; Zhan, Q.; Ouyang, W. Science of the Total Environment How to Quantify the Relationship between Spatial Distribution of Urban Waterbodies and Land Surface Temperature? *Sci. Total Environ.* **2019**, *671*, 1–9. [CrossRef] [PubMed]
- Guo, G.; Zhou, X.; Wu, Z.; Xiao, R.; Chen, Y. Characterizing the Impact of Urban Morphology Heterogeneity on Land Surface Temperature in Guangzhou, China. *Environ. Model. Softw.* **2016**, *84*, 427–439. [CrossRef]

13. He, B.J.; Zhu, J.; Zhao, D.X.; Gou, Z.H.; da Qi, J.; Wang, J. Co-Benefits Approach: Opportunities for Implementing Sponge City and Urban Heat Island Mitigation. *Land Use Policy* **2019**, *86*, 147–157. [[CrossRef](#)]
14. Badura, T.; Krkoška Lorencová, E.; Ferrini, S.; Vačkářová, D. Public Support for Urban Climate Adaptation Policy through Nature-Based Solutions in Prague. *Landsc. Urban Plan.* **2021**, *215*, 104215. [[CrossRef](#)]
15. Ouyang, W.; Morakinyo, T.E.; Ren, C.; Ng, E. The Cooling Efficiency of Variable Greenery Coverage Ratios in Different Urban Densities: A Study in a Subtropical Climate. *Build. Environ.* **2020**, *174*, 106772. [[CrossRef](#)]
16. Ghosh, S.; Das, A. Modelling Urban Cooling Island Impact of Green Space and Water Bodies on Surface Urban Heat Island in a Continuously Developing Urban Area. *Model. Earth Syst. Environ.* **2018**, *4*, 501–515. [[CrossRef](#)]
17. Kirschner, V.; Macků, K.; Moravec, D.; Mañas, J. Measuring the Relationships between Various Urban Green Spaces and Local Climate Zones. *Sci. Rep.* **2023**, *13*, 9799. [[CrossRef](#)] [[PubMed](#)]
18. Wang, Y.; Ouyang, W. Investigating the Heterogeneity of Water Cooling Effect for Cooler Cities. *Sustain. Cities Soc.* **2021**, *75*, 103281. [[CrossRef](#)]
19. Jacobs, C.; Klok, L.; Bruse, M.; Cortesão, J.; Lenzholzer, S.; Kluck, J. Are Urban Water Bodies Really Cooling? *Urban Clim.* **2020**, *32*, 100607. [[CrossRef](#)]
20. Lin, Y.; Wang, Z.; Jim, C.Y.; Li, J.; Deng, J.; Liu, J. Water as an Urban Heat Sink: Blue Infrastructure Alleviates Urban Heat Island Effect in Mega-City Agglomeration. *J. Clean. Prod.* **2020**, *262*, 121411. [[CrossRef](#)]
21. Agathangelidis, I.; Cartalis, C.; Santamouris, M. Urban Morphological Controls on Surface Thermal Dynamics: A Comparative Assessment of Major European Cities with a Focus on Athens, Greece. *Climate* **2020**, *8*, 131. [[CrossRef](#)]
22. Pang, B.; Zhao, J.; Zhang, J.; Yang, L. How to Plan Urban Green Space in Cold Regions of China to Achieve the Best Cooling Efficiency. *Urban Ecosyst.* **2022**, *25*, 1181–1198. [[CrossRef](#)]
23. Grilo, F.; Pinho, P.; Aleixo, C.; Catita, C.; Silva, P.; Lopes, N.; Freitas, C.; Santos-Reis, M.; McPhearson, T.; Branquinho, C. Using Green to Cool the Grey: Modelling the Cooling Effect of Green Spaces with a High Spatial Resolution. *Sci. Total Environ.* **2020**, *724*, 138182. [[CrossRef](#)]
24. Qiu, K.; Jia, B. The Roles of Landscape Both inside the Park and the Surroundings in Park Cooling Effect. *Sustain. Cities Soc.* **2020**, *52*, 101864. [[CrossRef](#)]
25. Ferreira, L.S.; Duarte, D.H.S. Exploring the Relationship between Urban Form, Land Surface Temperature and Vegetation Indices in a Subtropical Megacity. *Urban Clim.* **2019**, *27*, 105–123. [[CrossRef](#)]
26. Chen, W.; Zhang, J.; Shi, X.; Liu, S. Impacts of Building Features on the Cooling Effect of Vegetation in Community-Based Microclimate: Recognition, Measurement and Simulation from a Case Study of Beijing. *Int. J. Environ. Res. Public Health* **2020**, *17*, 8915. [[CrossRef](#)] [[PubMed](#)]
27. Straub, A.; Berger, K.; Breitner, S.; Cyrus, J.; Geruschkat, U.; Jacobeit, J.; Kühnbach, B.; Kusch, T.; Philipp, A.; Schneider, A.; et al. Statistical Modelling of Spatial Patterns of the Urban Heat Island Intensity in the Urban Environment of Augsburg, Germany. *Urban Clim.* **2019**, *29*, 100491. [[CrossRef](#)]
28. Xue, Z.; Hou, G.; Zhang, Z.; Lyu, X.; Jiang, M.; Zou, Y.; Shen, X.; Wang, J.; Liu, X. Quantifying the Cooling-Effects of Urban and Peri-Urban Wetlands Using Remote Sensing Data: Case Study of Cities of Northeast China. *Landsc. Urban Plan.* **2019**, *182*, 92–100. [[CrossRef](#)]
29. Zheng, Z.; Zhou, W.; Yan, J.; Qian, Y.; Wang, J.; Li, W. The Higher, the Cooler? Effects of Building Height on Land Surface Temperatures in Residential Areas of Beijing. *Phys. Chem. Earth* **2019**, *110*, 149–156. [[CrossRef](#)]
30. Rahman, M.M.; Avtar, R.; Yunus, A.P.; Dou, J.; Misra, P.; Takeuchi, W.; Sahu, N.; Kumar, P.; Johnson, B.A.; Dasgupta, R.; et al. Monitoring Effect of Spatial Growth on Land Surface Temperature in Dhaka. *Remote Sens.* **2020**, *12*, 1191. [[CrossRef](#)]
31. Yu, S.; Chen, Z.; Yu, B.; Wang, L.; Wu, B.; Wu, J.; Zhao, F. Exploring the Relationship between 2D/3D Landscape Pattern and Land Surface Temperature Based on Explainable EXTreme Gradient Boosting Tree: A Case Study of Shanghai, China. *Sci. Total Environ.* **2020**, *725*, 138229. [[CrossRef](#)]
32. He, B.J.; Wang, J.; Zhu, J.; Qi, J. Beating the Urban Heat: Situation, Background, Impacts and the Way Forward in China. *Renew. Sustain. Energy Rev.* **2022**, *161*, 112350. [[CrossRef](#)]
33. Alexander, C. Influence of the Proportion, Height and Proximity of Vegetation and Buildings on Urban Land Surface Temperature. *Int. J. Appl. Earth Obs. Geoinf.* **2021**, *95*, 102265. [[CrossRef](#)]
34. COM. *Green Paper on the Urban Environment*; Commission of the European Communities: Luxembourg, 1990.
35. Štěpánek, P.; Trnka, M.; Meitner, J.; Dubrovský, M.; Zahradníček, P.; Lhotka, O.; Skalák, P.; Kyselý, J.; Farda, A.; Semerádová, D. *Očekávané Klimatické Podmínky v České Republice Část I. Změna Základních Parametrů*; Czech Globe: Brno, Czech Republic, 2019.
36. ČHMÚ. *Výroční Zpráva ČHMÚ*; ČHMÚ: Prague, Czech Republic, 2019.
37. Ouředníček, M.; Pospíšilová, L.; Špačková, P.; Temelová, J.; Novák, J. Prostorová Typologie a Zonace Prahy. In *Sociální Proměny Pražských Čtvrtí (Social Change of the Cities)*; Ouředníček, M., Temelová, J., Eds.; Academia: Prague, Czech Republic, 2012; pp. 268–286.
38. Yang, Q.; Huang, X.; Tang, Q. The Footprint of Urban Heat Island Effect in 302 Chinese Cities: Temporal Trends and Associated Factors. *Sci. Total Environ.* **2019**, *655*, 652–662. [[CrossRef](#)]
39. van de Griend, A.A.; Owe, M. On the Relationship between Thermal Emissivity and the Normalized Difference Vegetation Index for Natural Surfaces. *Int. J. Remote Sens.* **1993**, *14*, 1119–1131. [[CrossRef](#)]

40. Asgarian, A.; Amiri, B.J.; Sakieh, Y. Assessing the Effect of Green Cover Spatial Patterns on Urban Land Surface Temperature Using Landscape Metrics Approach. *Urban Ecosyst.* **2015**, *18*, 209–222. [[CrossRef](#)]
41. Cooley, T.; Anderson, G.P.; Felde, G.W.; Hoke, M.L.; Ratkowski, A.J.; Chetwynd, J.H.; Gardner, J.A.; Adler-Golden, S.M.; Matthew, M.W.; Berk, A.; et al. FLAASH, a MODTRAN4-Based Atmospheric Correction Algorithm, Its Application and Validation. In Proceedings of the IEEE International Geoscience and Remote Sensing Symposium, Toronto, ON, Canada, 24–28 June 2002; Volume 3, pp. 1414–1418.
42. Azen, R.; Budescu, D.V. The Dominance Analysis Approach for Comparing Predictors in Multiple Regression. *Psychol. Methods* **2003**, *8*, 129–148. [[CrossRef](#)]
43. Karimi Firozjaei, M.; Kiavarz, M.; Alavipanah, S.K. Impact of Surface Characteristics and Their Adjacency Effects on Urban Land Surface Temperature in Different Seasonal Conditions and Latitudes. *Build. Environ.* **2022**, *219*, 109145. [[CrossRef](#)]
44. Kovář, P. *Ekosystémová a Krajinná Ekologie*; Charles University, Karolinum: Prague, Czech Republic, 2014; ISBN 978-80-246-2788-5.
45. Zhang, Z.; Paschalis, A.; Mijic, A.; Meili, N.; Manoli, G.; van Reeuwijk, M.; Fatichi, S. A Mechanistic Assessment of Urban Heat Island Intensities and Drivers across Climates. *Urban Clim.* **2022**, *44*, 101215. [[CrossRef](#)]
46. Fedor, T.; Hofierka, J. Comparison of Urban Heat Island Diurnal Cycles under Various Atmospheric Conditions Using WRF-UCM. *Atmosphere* **2022**, *13*, 2057. [[CrossRef](#)]
47. Chen, J.; Zhan, W.; Du, P.; Li, L.; Li, J.; Liu, Z.; Huang, F. Seasonally Disparate Responses of Surface Thermal Environment to 2D / 3D Urban Morphology. *Build. Environ.* **2022**, *214*, 108928. [[CrossRef](#)]
48. Anselin, L. Spatial Econometrics. In *A Companion to Theoretical Econometrics*; Baltagi, B.H., Ed.; Blackwell Publishing Ltd.: Hoboken, NJ, USA, 2003.
49. Anselin, L. *Spatial Econometrics: Methods and Models*, 1st ed.; Springer: Dordrecht, The Netherlands, 1988.
50. Brunson, C.; Fotheringham, S.; Charlton, M. Geographically Weighted Regression. *J. R. Stat. Soc. Ser. D (Stat.)* **1998**, *47*, 431–443. [[CrossRef](#)]
51. Brunson, C.; Fotheringham, A.S.; Charlton, M.E. Geographically Weighted Regression: A Method for Exploring Spatial Nonstationarity. *Geogr. Anal.* **1996**, *28*, 281–298. [[CrossRef](#)]
52. Stewart, I.D.; Oke, T.R. Local Climate Zones for Urban Temperature Studies. *Bull. Am. Meteorol. Soc.* **2012**, *93*, 1879–1900. [[CrossRef](#)]

Disclaimer/Publisher’s Note: The statements, opinions and data contained in all publications are solely those of the individual author(s) and contributor(s) and not of MDPI and/or the editor(s). MDPI and/or the editor(s) disclaim responsibility for any injury to people or property resulting from any ideas, methods, instructions or products referred to in the content.